Macromolecules

Article

pubs.acs.org/Macromolecules

Detection of Radicals by Spin Trapping ESR in a Fuel Cell Operating with a Sulfonated Poly(ether ether ketone) (SPEEK) Membrane

Marek Danilczuk,[†,§] Shulamith Schlick,*[,†] and Frank D. Coms[‡,∥]

[†]Department of Chemistry and Biochemistry, University of Detroit Mercy, 4001 West McNichols, Detroit, Michigan 48221, United States

[‡]General Motors Electrochemical Energy Research Lab, 10 Carriage Street, Honeoye Falls, New York 14472, United States

ABSTRACT: We present experiments in a fuel cell (FC) inserted in the resonator of the electron spin resonance (ESR) spectrometer, which allowed separate monitoring of radical formation at anode and cathode sides. The *in situ* FC was operated at 300 K under closed- and open-circuit voltage conditions, CCV and OCV, respectively, with a membrane–electrode assembly (MEA) based on sulfonated poly(ether ether ketone) (SPEEK). The formation of radicals was monitored by spin trapping ESR, with 5,5-dimethyl-1-pyrroline *N*-oxide (DMPO) as the spin trap. The magnetic parameters and the relative intensities of DMPO adducts were determined by simulation of the ESR spectra. The major adducts detected at both electrodes were DMPO/OOH and DMPO/H. The generation of the DMPO/OOH adduct at the anode can be explained by reaction of crossover oxygen with hydrogen atoms formed at the Pt catalyst; at the cathode this adduct can be generated by H_2 crossover to the cathode, reaction at the Pt catalyst, and reaction with O_2. The generation of the DMPO/OOH adduct depends therefore on gas crossover: at the anode from crossover O_2 and at the cathode from crossover H_2. Results indicated that the crossover rates are enhanced in the more highly hydrated membrane. No membrane-derived carbon-centered or oxygen-centered radical adducts were detected in the *in situ* FC. However, in SPEEK membranes directly exposed to hydroxyl radicals in the presence of DMPO, the DMPO/Ph and DMPO/OPh adducts were detected, indicating poor chemical stability of SPEEK in the *ex situ* Fenton test. The conclusion is that hydrocarbon membranes such as SPEEK demonstrate different chemical stabilities in the two tests.

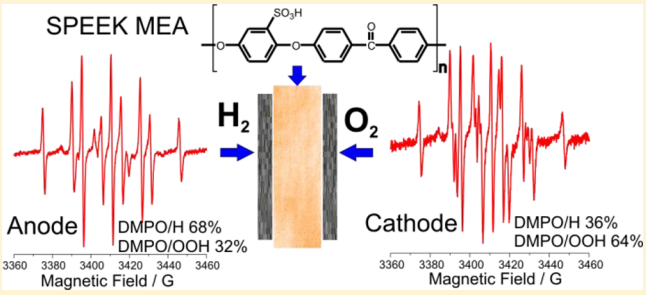

INTRODUCTION

Proton-exchange membrane fuel cells (PEMFCs) operating around 80 °C have attracted considerable interest because of their potential as energy converters for transportation, stationary, and portable applications. Important components of a PEMFC are the catalyst, the proton exchange membrane (PEM), and the fuel (hydrogen or, in some cases, methanol). The role of the membrane is crucial: to separate the cathode and anode compartments and to allow efficient proton transport from the anode to the cathode. PEM is an ionomer, a polymer modified to include ions, typically sulfonic acid groups. The most commonly used PEMs for hydrogen and direct methanol fuel cells are perfluorosulfonic acid ionomers (PFSA) based on a Teflon-like backbone with side chains containing sulfonic groups; examples include Nafion, Aquivion, and 3M membranes.[1,2] These materials exhibit excellent mechanical, chemical, and thermal stability in both oxidative and reductive media, and their performance is close to current Department of Energy (DOE) requirements for automotive applications. However, some problems remain, among them high cost of the membrane and catalyst, low oxygen reduction rate (ORR) at the low pH, and high gas crossover, hydrogen to the cathode and oxygen to the anode.[3]

These drawbacks led to intense activity in the research and development of alternative, nonfluorinated, PEMs. Several aromatic homopolymers and copolymers with pendant ionic groups, such as sulfonated poly(arylene ether),[4,5] polysulfone,[6] sulfonated poly(benzoyl paraphenylene),[7] polybenzimidazole,[8] and sulfonated poly(arylene ether sulfone),[9,10] have good thermo-oxidative stability and excellent mechanical properties along with high proton conductivity. Because of their properties and low cost, poly(arylene ether)-based sulfonated polymers are considered as potential candidates for FC applications.

Membrane durability is a critical issue in fuel cell systems and is usually assessed by a combination of *ex situ* methods, such as the Fenton test, and *in situ* measurement of accelerated lifetime, open circuit voltage (OCV) decay, and potential cycling. The behavior of PFSA membranes has been extensively studied and summarized, and the relationship between *ex situ* and *in situ* results has been discussed in detail.[3] Our work has resulted in the visualization of chemical and crossover processes in a FC inserted in the ESR resonator and in-depth profiling of degradation by 2D spectral-spatial FTIR;[11−14] these and

Received: June 10, 2013
Revised: July 13, 2013
Published: July 25, 2013

other important papers[15−19] have demonstrated that a combination of spectroscopic and other methods can provide valuable information on the location of membrane degradation sites, on the spatial distribution of functional groups over the degraded area, and on the mechanism of membrane degradation and stabilization in operating FCs.

The results for hydrocarbon-based membranes, in particular for aromatic homopolymers and copolymers, have been discussed by Gittleman et al.[19] in terms of their stability in *ex situ* and *in situ* experiments. An important observation was that some of these membranes show poor stability in the Fenton test (in the presence of hydroxyl radicals), but great stability in FC environments, leading to the conclusion that the chemical durability of hydrocarbon membranes "requires a paradigm that is distinct from that used for PFSAs". Lower crossover rates of the gases have been suggested as an important reason for the greater stability of aromatic membranes in a FC.

Sulfonated poly(ether ether ketone) (SPEEK) (Chart 1) is a promising ionomer for PEMFCs applications.[20−22] The proton

Chart 1. Repeat Unit of Sulfonated Poly(ether ether ketone) (SPEEK)

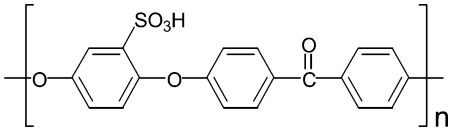

conductivity and swelling properties of SPEEK membranes with 50−70% degree of sulfonation (DS) are comparable to Nafion at room temperature and can be controlled by the DS.[23] However, membranes with DS of 50% dissolve in water at temperatures above 80 °C.[24,25]

SPEEK membranes are usually prepared by casting from solutions using solvents such as *N,N*-dimethylformamide, *N,N*-dimethylacetamide, dimethyl sulfoxide, or *N*-methyl-2-pyrrolidinone. Although several studies on the SPEEK as a PEM in both hydrogen and direct methanol fuel cells have been conducted, discrepancies have been reported between data for proton conductivity, water uptake, cell performance, and morphology of SPEEK membranes obtained in different laboratories.[26−29] Even with a similar degree of sulfonation, SPEEK conductivity differs, probably due to the different solvent used during membrane preparation, as each solvent can interact differently with the SPEEK sulfonic groups. The strong interaction of *N,N*-dimethylformamide and *N,N*-dimethylacetamide decreases the number and mobility of protons and leads to significant reduction of conductivity.[22,30] In addition, SPEEK-based membranes are susceptible to hydroxyl radical-initiated degradation,[31−34] and some degradation was reported during FC tests.[35] Extensive efforts were made to improve membrane properties by cross-linking[36,37] and grafting.[38,39]

In our laboratory we have developed spin trapping ESR methods for visualizing the presence of short-lived radicals generated during the fragmentation of perfluorinated and hydrocarbon membranes. The method is based on scavenging of short-lived radicals by spin traps and formation of more stable spin adducts, typically nitroxide radicals, as shown in Scheme 1 for the nitrone spin trap 5,5-dimethyl-1-pyrroline *N*-oxide (DMPO). In most cases the ESR spectra of spin adducts of nitrone spin traps exhibit hyperfine splittings (hfs) from ^{14}N and H_β nuclei.[40] From these parameters it is often possible to determine the identity of trapped radicals.

Scheme 1. 5,5-Dimethyl-1-pyrroline *N*-Oxide (DMPO) Spin Trapping Reaction

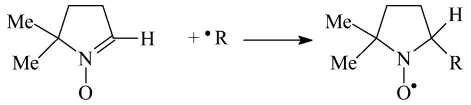

DMPO Spin Trap DMPO/R adduct

Our *ex situ* study of SPEEK membranes and low-molecular-weight model compounds exposed to HO• radicals, using both direct ESR and spin trapping ESR methods, has shown the presence of phenoxyl and phenyl radicals and provided evidence that HO• radical attack leads to the scission of the ether bridge in the membrane backbone.[32]

The goal of the present study was to identify short-lived fragments as spin adducts separately at the cathode and anode, to compare with the behavior of Nafion membranes in similar experiments, and to compare SPEEK fragmentation in an operating FC with the published *ex situ* experiments.[32] The presence of radicals was determined by ESR spin trapping. DMPO was the spin trap of choice in this study because of its ability to distinguish between carbon-centered radicals (CCRs) and oxygen-centered radicals (OCR). These experiments allowed us to detect *separately* radicals formed at both electrodes during CCV and OCV FC operation. As shown below, important differences were detected between *ex situ* and *in situ* results, the major difference being the absence of SPEEK-derived radical adducts in an operating FC. In addition, this study has emphasized the importance of crossover processes and their dependence on the membrane degree of hydration.

EXPERIMENTAL SECTION

Materials. DMPO was purchased from Enzo Life Science Inc. and used without further purification. The gases (H_2 99.99%, O_2 99.6%), Pt mesh with d = 0.1 mm, and Ag wire with d = 0.127 mm were from Sigma-Aldrich. The SPEEK membrane was cast from a dimethylformamide (DMF) solution. Membrane-electrode assemblies (MEAs) based on SPEEK membranes of thickness 50 μm were from Cortney Mittelsteadt of Giner Electrochemical Systems, LLC, where Pt black electrodes were applied using the decal-transfer process. The ionic exchange capacity (IEC) was 2.0 mequiv g^{-1}, corresponding to DS = 70%. The λ values for the dry and water-saturated membranes were 1 (3.6 wt % water) and 4.7 (17.0 wt % water), respectively. The catalyst coverage was 0.2 mg cm^{-2}. The *in situ* FC consists of two half-cylinders made of cross-linked polystyrene (Rexolite), with indentation where the membrane, the Pt mesh, and the electrodes were placed.[12,13] The FC was placed in the variable-temperature insert of the ESR spectrometer. The gas flows to the FC, 2 cm^3 min^{-1} for oxygen and 4 cm^3 min^{-1} for hydrogen, were controlled with OMEGA FMA-2603A mass flow controllers.

Spin Trapping. Because of the very low concentration and limited stability of generated radicals, spin trapping ESR was used to scavenge the radicals; DMPO was chosen as a spin trap because of its well-documented trapping ability for trapping of various radical types.[11−14] About 1 μL of the aqueous solution of the spin trap, concentration 4 M, was deposited at the cathode or anode side just before starting the FC operation. The cell voltage was 0.6−0.7 V, and the temperature was maintained at 300 K. Our previous study had showed that deposition of the spin trap separately at one electrode leads to the trapping radicals *only* at that electrode. No signals were detected before connecting the gases and deposition of the spin trap on the membrane or in the presence of the spin trap and the absence of the gases.

ESR Measurements. ESR spectra were recorded using the Bruker X-band EMX spectrometer operating at 9.7 GHz and 100 kHz magnetic field modulation and equipped with the Acquisit 32 Bit

dx.doi.org/10.1021/ma401188u | *Macromolecules* 2013, 46, 6110−6117

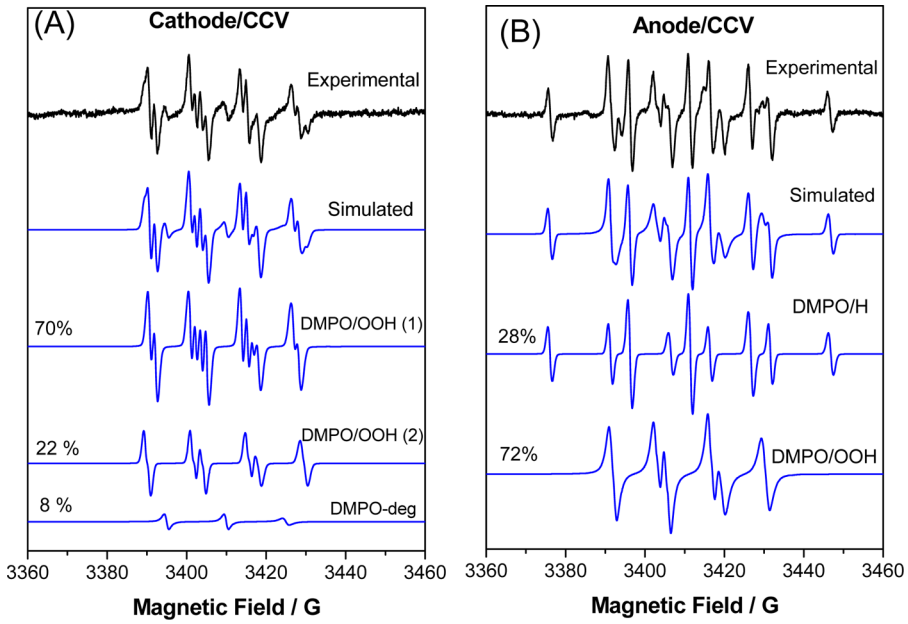

Figure 1. Experimental and simulated ESR spectra of the DMPO adducts observed in FC operated at CCV with dry MEA and spin trap deposited at the cathode (A) and the anode (B). The initial water content in the membrane was 3.6 wt %. Modulation amplitude 1 G, receiver gain 1×10^5, 16 scans. (All experimental ESR spectra are in black, and all simulated spectra are in blue.)

Table 1. Hyperfine Splittings and Relative Intensities of DMPO Adducts Detected in the *in Situ* FC Operated with Dry and Wet SPEEK MEAs

			hyperfine splittings (G)			
water content (wt %)	system	adduct	a_N	$a_{H\beta}$	$a_{H\gamma}$	rel int (%)
3.6	cathode/CCV	DMPO/OOH (1)	12.9	10.2	1.4	70
	(Figure 1A)	DMPO/OOH (2)	13.9	12.6	1.0	22
		DMPO-deg	15.0			8
	anode/CCV	DMPO/H	15.2	20.1 (2H)		28
	(Figure 1B)	DMPO/OOH	13.6	11.5	NR[a]	72
	cathode/OCV	DMPO/H	14.9	19.9 (2H)		60
	(Figure 2A)	DMPO/OOH	13.0	10.6	1.3	40
	anode/OCV	DMPO/H	14.9	19.9 (2H)		78
	(Figure 2B)	DMPO/OOH	13.2	10.6	1.2	22
17.0	cathode/CCV	DMPO/H	15.4	20.6 (2H)		36
	(Figure 3A)	DMPO/OOH	13.2	10.4	1.4	64
	anode/CCV	DMPO/H	15.2	20.3 (2H)		68
	(Figure 3B)	DMPO/OOH	13.6	10.9	1.2	32
	cathode/OCV	DMPO/H	14.9	19.9 (2H)		59
	(Figure 4A)	DMPO/OOH	13.0	10.3	1.4	41
	anode/OCV	DMPO/H	15.0	20.0 (2H)		60
	(Figure 4B)	DMPO/OOH	12.9	10.2	1.4	40

[a]Not resolved.

WINEPR data system version 4.33 rev.04 for acquisition and manipulation and with the ER 4111 VT variable-temperature unit. The microwave frequency was measured with the Agilent 53150A microwave frequency counter. The hfs of the spin adducts were determined by fitting the spectra using the WinSim (NIEHS/NIH) simulation package with automatic fitting of the isotropic spectra from the adducts, followed by manual variation of the magnetic parameters;[41] spectra simulation also determined the relative intensity of each component for spectra that consisted of a superposition of contributions from different components. Typical acquisition parameters for the ESR spectra were sweep width 150 G, microwave power 2 mW, time constant 20.48 ms, conversion time 41.94 ms, 2048 points, modulation amplitude 1 G, and receiver gain 1×10^5. The number of scans was 16 for spectra in Figure 1 and 64 for the other spectra.

Two MEAs with different initial levels of hydration were used in this study: the "dry" MEA stored in air contained 3.6 wt % water; the "wet" MEA stored in deionized water contained 17.0 wt % water. The hydration level increases during FC operation; therefore, the water contents given above refer to the *initial* amount of water in the MEA, before fuel cell operation in the presence of the spin trap. However, we do not expect that the final water uptake of the MEAs exceed 17.0 wt %, the amount determined in the "wet" MEA. The terms *dry* and *wet* used in the text refer to MEAs with water contents of 3.6 or 17.0 wt %, respectively.

RESULTS

In this section we will present the ESR spectra of DMPO adducts generated for the "dry" and "wet" SPEEK MEAs, in

dx.doi.org/10.1021/ma401188u | *Macromolecules* 2013, 46, 6110−6117

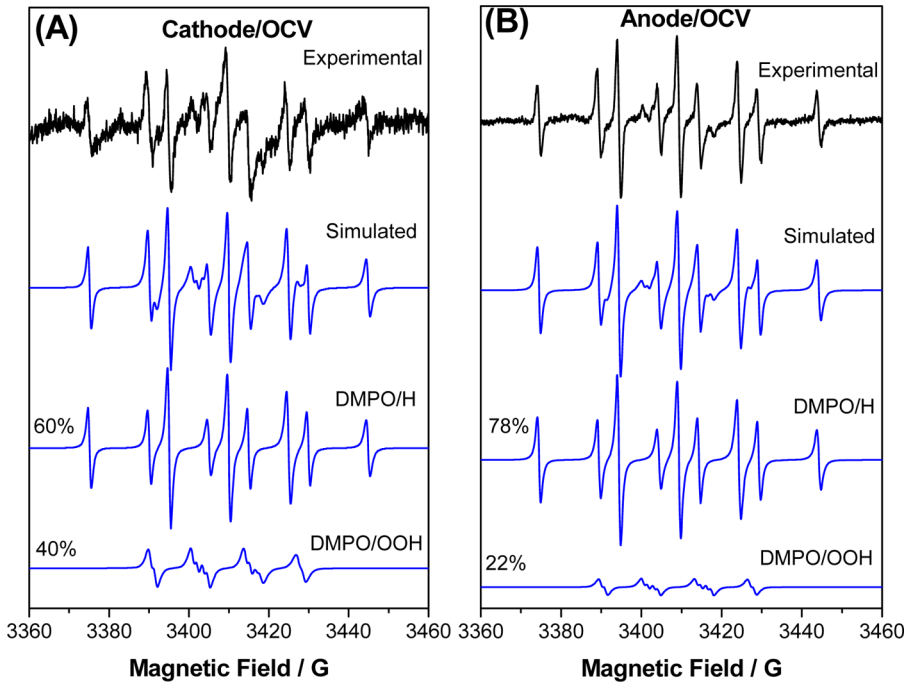

Figure 2. Experimental and simulated ESR spectra of the DMPO adducts observed in FC with a dry MEA operated at OCV conditions with spin trap deposited at the cathode (A) and the anode (B). The initial water content in the membrane was 3.6 wt %. Modulation amplitude 1 G, receiver gain 1×10^5, 64 scans.

CCV and OCV conditions. The assignment of a spectral component to a spin adduct is based on a careful investigation of the spin trapping literature[42−45] and the identification of adducts presented in our papers.[11−13] The magnetic parameters and relative intensities of spin adducts observed in the present study are summarized in Table 1.

Dry MEA, CCV. ESR spectra of DMPO adducts detected at both electrodes in the FC with SPEEK MEAs are presented in Figure 1. Figure 1A presents experimental and simulated ESR spectra detected when the spin trap was deposited at the cathode side. The experimental spectrum was simulated by a sum of three components: The dominating adduct, 70% of the total intensity, was simulated with a_N = 12.9 G, $a_{H\beta}$ = 10.2 G, and $a_{H\gamma}$ = 1.4 G, and assigned to the DMPO/OOH (1) adduct. The second component, 22% of the total intensity, was simulated with a_N = 13.9 G, $a_{H\beta}$ = 12.6 G, and $a_{H\gamma}$ = 1.0 G and assigned to the DMPO/OOH (2). The third component, a weak triplet with a_N = 15 G and 8% of total intensity, was assigned to the degraded spin trap; this adduct has a low relative intensity and can usually be identified only when no spectral contributions from the other components appear in the *center* of the ESR spectrum.[11,46] When the gas flows were stopped, the signals from both DMPO/OOH adducts could still be observed for about 30 min. Despite the superposition of three spectral components, experimental and simulated spectra are in excellent agreement. The identification of *two* adducts of the hydroperoxy radical HOO$^\bullet$ is based on different a_N values, 12.9 and 13.9 G, respectively. The a_N values are expected to depend on the local polarity and are often assigned to the same nitroxide radicals in media of different polarity: For di-*tert*-butyl nitroxide (DTBN), the a_N values were 17.1 G in a polar solvent and 16.6 G when included inside the hydrophobic host *β*-cyclodextrin;[47] the corresponding a_N values in the host cucurbituril 7 (CB[7]) were 17.1 and 15.5 G, in agreement with the higher expected host hydrophobicity.[48] Two DMPO/OOH adducts were detected only in the drier SPEEK and seem to signal partition of the adduct in a phase-separated membrane. It is also clear that different adduct locations also affect the corresponding a_H values and may lead to different trapping rates and possibly to different signal intensities of the spin adducts. It is important to note that multiscale simulations of hydrated SPEEK membranes with λ values in the range 10−20 have indicated the presence of phase separation into hydrophobic and hydrophilic domains;[49] the water channels in SPEEK seem to be narrower that in Nafion. In addition, a spin probe study of hydrated SPEEK has shown that the spin probe occupies two locations with different polarity and dynamics.[50]

The ESR spectra recorded when the spin trap was added at the anode and the FC was operated at CCV conditions are presented in Figure 1B. The simulated spectrum was deconvoluted into two components. The major component was assigned to the DMPO/OOH adduct with a_N = 13.6 G and $a_{H\beta}$ = 11.5 G and 72% of the total ESR intensity; the $a_{H\gamma}$ splitting was not resolved. The additional component, with a_N = 15.2 G and a_H = 20.1 G (2H) and 28% of the total intensity, was assigned to DMPO/H; we note that this adduct was not detected at the cathode (Figure 1A). When the gas flows were stopped, the signal from DMPO/OOH adduct disappeared after ≈30 min, but the DMPO/H adduct was still detected after ≈1 h.

Dry MEA, OCV. The ESR spectra obtained for the *in situ* FC operated at OCV conditions are presented in Figure 2. Figure 2A presents experimental and simulated ESR spectra observed when the spin trap was placed at the cathode side. The weak experimental spectrum was simulated in the terms of two components. The dominating signal, with 60% of the total intensity, was assigned to the DMPO/H adduct and simulated with a_N = 14.9 G and a_H = 19.9 G (2H), close to the hfs deduced for this adduct in the Nafion MEA.[12] The second component, with 40% of the total intensity, exhibits an ESR

dx.doi.org/10.1021/ma401188u | *Macromolecules* 2013, 46, 6110−6117

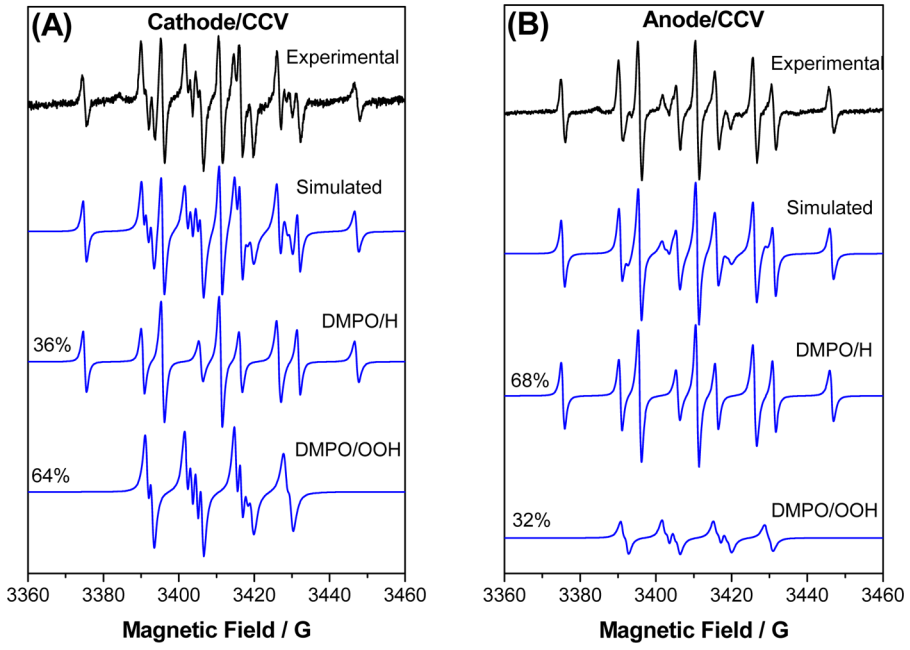

Figure 3. Experimental and simulated ESR spectra of the DMPO adducts observed in FC operated at CCV with wet MEA and spin trap at the cathode (A) and at the anode (B). The initial water content in the membrane was 17.0 wt %. Modulation amplitude 1 G, receiver gain 1×10^5, 64 scans.

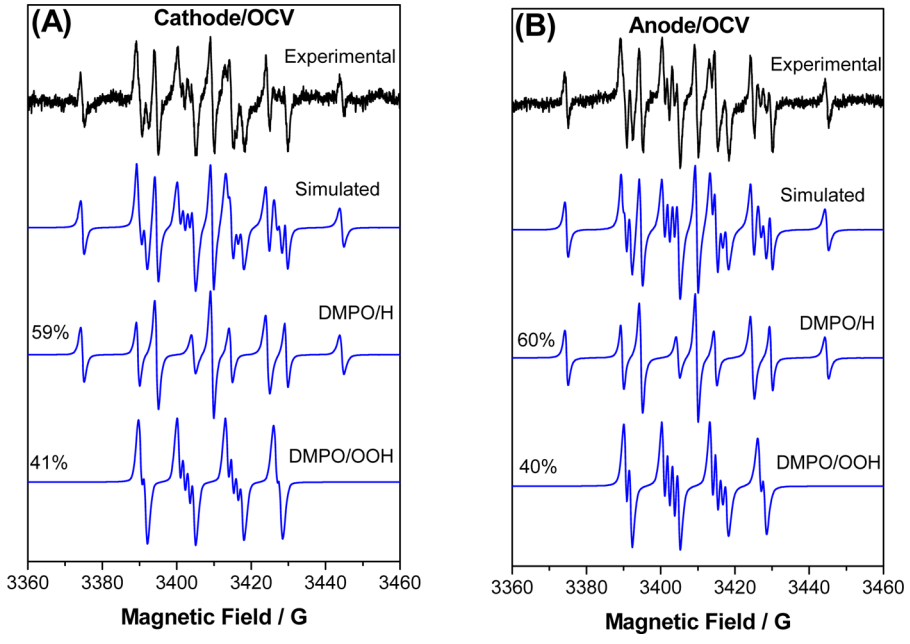

Figure 4. Experimental and simulated ESR spectra of the DMPO adducts observed in FC operated at OCV with wet MEA and spin trap deposited at the cathode (A) and the anode (B). The initial water content in the membrane was 17.0 wt %. Modulation amplitude 1 G, receiver gain 1×10^5, 64 scans.

spectrum typical for DMPO/OOH and was simulated with a_N = 13.0 G, $a_{H\beta}$ = 10.6 G, and $a_{H\gamma}$ = 1.3 G. All signals disappeared ≈30 min after stopping the flow of gases to the FC.

The spectrum detected at the anode is similar to that at the cathode, but the signal intensity is significantly higher. The experimental and the simulated ESR spectra are presented in Figure 2B. The simulated spectrum consisted of two components. The contribution of DMPO/H is 78% of total intensity, and the signal was simulated with a_N = 14.9 G and a_H = 19.9 G (2H). The second component, with 22% of the total intensity, was assigned to DMPO/OOH and simulated with a_N = 13.2 G, $a_{H\beta}$ = 10.6 G, and $a_{H\gamma}$ = 1.2 G. After stopping the flow of gases, the signal of DMPO/OOH disappeared after ≈30 min, while the spectrum of DMPO/H was still observed after ≈1 h.

Wet MEA, CCV. Experimental and simulated ESR spectra obtained for the FC operated at CCV conditions in the SPEEK MEA with initial water content of 17.0 wt % are presented in Figure 3. Figure 3A shows the results observed at the cathode: The experimental spectrum was simulated in the terms of two

dx.doi.org/10.1021/ma401188u | *Macromolecules* 2013, 46, 6110–6117

components, DMPO/H with a_N = 15.4 G and a_H = 20.6 G (2H), and DMPO/OOH with a_N = 13.2 G, $a_{H\beta}$ = 10.4 G, and $a_{H\gamma}$ = 1.4 G. Their contribution to the total spectral intensity was 36% and 64%, respectively. In contrast to the spectra observed in the FC operated with the *drier* MEA, only *one* DMPO/OOH adduct was detected in the *wet* MEA; it is reasonable to assume that the higher water content may lead to dynamical averaging of the two sites. A strong signal of the DMPO/H adduct, 36% of the total intensity, was also detected.

Similar signals were also detected at the anode side, as seen in Figure 3B. The experimental spectrum was simulated as a sum of two adducts: DMPO/H with a_N = 15.2 G and a_H = 20.3 G (2H) and DMPO/OOH with a_N = 13.6 G, $a_{H\beta}$ = 10.9 G, and $a_{H\gamma}$ = 1.2 G. The contribution of the DMPO/H signal is much higher than at the cathode, 68% vs 36%.

Wet MEA, OCV. Figure 4 shows experimental and simulated ESR spectra for the *in situ* FC operated with the wet MEA at OCV conditions. In these experiments the same adducts, DMPO/H and DMPO/OOH, were observed at both electrodes, with almost identical relative intensities.

DISCUSSION

In this section we will discuss the generation and identification of the DMPO/H and DMPO/OOH adducts, the unexpected absence of the DMPO/OH adduct, comparison of present results with *ex situ* results on SPEEK membranes,[32] and the dominant role of crossover processes in the generation of unstable intermediates in the SPEEK FC.

The DMPO/H Adduct. The identification of DMPO/H is based on our previous studies, where the presence of this adduct was detected at both electrodes.[12,13] Several observations related to this adduct are important: In the present study the DMPO/H adduct was *not* detected for the drier membrane at the cathode/CCV (Figure 1A) but appeared in the wet membrane at the cathode/CCV (Figure 3A) and in all other spectra. The intensity of the ESR spectra was lower in the dry membrane at the cathode but much higher at the anode. In all samples, wet and dry, the relative intensity of DMPO/H was higher at the anode than at the cathode. These observations suggest the preferential generation of this adduct at the anode, leading us to propose the formation of $H^\bullet$ at the anode from the reaction of molecular hydrogen on the surface of the Pt catalyst, reaction 1, followed by spin trapping.

$$H_2 \rightarrow 2H^\bullet \quad \text{(at the Pt catalyst)} \qquad (1)$$

The appearance of DMPO/H at the cathode can be explained by hydrogen crossover from the anode to the cathode and formation of $H^\bullet$ at the surface of cathode Pt catalyst. The absence of this adduct at the cathode for the dry membrane, containing 3.6 wt % water, suggests a lower crossover rate in the dry membrane and will be discussed below.

The DMPO/OOH Adduct. This adduct is characterized by a 12-line ESR spectrum with typical hyperfine splittings $a_N \approx$ 14 G, $a_{H\beta} \approx$ 11 G, and $a_{H\gamma} \approx$ 1.3 G (1H).[43−45] However, some published data have suggested that the 12-line spectrum results from an overlap of two 6-line signals.[51] The ESR spectrum observed for the FC with the spin trap at the cathode and operated at CCV (Figure 1A) consists of more than 12 lines and was simulated as a superposition of *two* DMPO/OOH signals with slightly different hyperfine splittings, a result that may suggest two species in locations of different polarities in a phase-separated system, with a_N values of 12.9 and 13.9 G.

The DMPO/OOH adduct was detected with various relative intensities at both electrodes and for CCV and OCV operating conditions. The generation of this adduct at the cathode may be rationalized by H_2 crossover to the cathode, reaction at the Pt catalyst (1), and reaction (2) with O_2. This conclusion implies that $H^\bullet$ reacts faster with O_2 than with DMPO, a plausible assumption.[52]

$$H^\bullet + O_2 \rightarrow HOO^\bullet \qquad (2)$$

We must also consider the possibility that, under CCV conditions, DMPO/OOH can also be generated via the electrochemically formed H_2O_2, followed by reaction at the Pt catalyst; moreover, the supply of hydrogen atoms can be provided by protons. These processes could produce more $HOO^\bullet$ radicals than from crossover and may explain the higher DMPO/OOH adduct intensity under CCV conditions.

The DMPO/OOH adduct was also detected at the anode side. The presence of this adduct can be explained by reaction of crossover oxygen with hydrogen atoms formed at the anode Pt catalyst, reaction 1. At OCV conditions the generation of the DMPO/OOH adduct depends therefore on gas crossover: at the cathode from crossover H_2 and at the anode from crossover O_2. It is important to mention that a strong effect of membrane thickness was detected in our *in situ* ESR study of MEAs based on 3M membranes:[53] For a membrane thickness of 25 μm, the relative intensities of the DMPO/H and DMPO/OOH adducts were not too different, 55% and 45%, respectively, at both anode and cathode, and for OCV and CCV operations. For a thickness of 100 μm the relative intensity of the DMPO/H adduct at the cathode decreased significantly, a result explained by decreased H_2 crossover rate. At the anode DMPO/H was the only adduct detected; the absence of the DMPO/OOH adduct in the thickest membrane was assigned to negligible O_2 crossover in the thick membranes.

The effect of the water content on the number of DMPO/OOH adducts (two for dry MEAs and one only for MEA containing 17 wt % water) and on their magnetic parameters (especially on the value of a_N) will be further investigated by spin probe ESR: by examining the ESR spectra of a nitroxide probe, for example DTBN, in SPEEK membranes as a function of temperature and water content, in order to understand the effect of hydration on the self-assembling of the membrane and its dynamics. The *two* a_N values measured for the dry membrane may be due to the same nitroxide radicals located in media of different polarity. The single value for a_N measured in the wet membrane may be a result of rapid exchange between two sites. Therefore, the proposed study is expected to clarify both the polarity distribution in the membrane, and the local dynamics.[54]

The Absence of the DMPO/OH Adduct. Our previous *in situ* FC study with Nafion-based MEAs showed that the hydroxyl radical is a major species formed at the cathode side for CCV conditions.[12] In contrast to this study, the DMPO/OOH adduct is dominant in the ESR spectra observed at the cathode side. $HOO^\bullet$ radicals at the cathode can be formed from electrochemically generated H_2O_2 (3), followed by reactions 4 and 5. The detection of DMPO/OOH at the cathode under OCV conditions may imply that the $HO^\bullet$ radical is formed chemically at the catalyst but reacts with the aromatic rings via addition reactions: As described in ref 19, the reaction of the $HO^\bullet$ radical with the aromatic ring is faster than with H_2, and the radical generated may be involved in quenching reactions before being trapped by DMPO.

dx.doi.org/10.1021/ma401188u | *Macromolecules* 2013, 46, 6110−6117

$$O_2 + 2H^+ + 2e^- \rightarrow H_2O_2$$

(electrochemical route of H_2O_2 formation) (3)

$$H_2O_2 \rightarrow 2HO^\bullet \quad (4)$$

$$H_2O_2 + HO^\bullet \rightarrow HOO^\bullet + H_2O \quad (5)$$

We note that the DMPO/OH adduct was detected at cathode OCV in the *in situ* ESR study of sulfonated poly(benzoyl paraphenylene) (SParmax).[7] It is possible that the diffusion-controlled reaction of $HO^\bullet$ with SParmax is slower than the corresponding reaction in SPEEK (for the experimental conditions described above).

Comparing *ex Situ* and *in Situ* Results for SPEEK. In SPEEK membrane directly exposed to hydroxyl radicals and in the presence of DMPO, the adducts detected were DMPO/Ph and DMPO/OPh,[31,32] indicating poor chemical stability of SPEEK in a Fenton test; Ph is the phenyl radical, and OPh is the phenoxyl radical. In contrast to these *ex situ* experiments, no membrane-derived radical adducts were detected in the *in situ* FC. These results are similar to those presented for SParmax[7] and are in accord with ideas presented in ref 19, as mentioned in the Introduction. We recall that, in the case of Nafion, we have detected the membrane-derived radical adduct after 120 min of FC operation.[12] This type of experiment was not possible with SPEEK because even after 1 h of FC operation the membrane became soft as a gel, a sign of incipient dissolution in water.

The Dominant Role of Crossover Processes in the Generation of Unstable Intermediates. As described above, the generation of the DMPO/OOH adduct depends on gas crossover, at the cathode from H_2 crossover, and at the anode from O_2 crossover. In addition, gas crossover seems to be faster in the wet MEA, as seen in the results shown in Figure 4: The same adducts were observed at both electrodes, with almost identical relative intensities. We note that a significant increase of gas diffusion in hydrated Nafion was reported and explained by gas circulation through the hydrated hydrophilic ionic clusters.[54,55] We emphasize that gas crossover is expected to depend on membrane thickness.[53] The results presented here are for a membrane thickness of 50 μm.

■ CONCLUSIONS

We have presented the detection of short-lived radical intermediates generated in a fuel cell inserted in the resonator of the ESR spectrometer, as adducts of the spin trap 5,5-dimethyl-1-pyrroline *N*-oxide (DMPO). The FC used MEAs based on sulfonated poly(ether ether ketone) (SPEEK) membranes with thickness of 50 μm and coated with Pt as catalyst. By selecting the electrode where the spin trap was deposited, the experiments allowed monitoring of radical formation separately at each electrode. All radicals, identified as spin adducts, were trapped in the early stage of FC operation.

The major adducts detected were DMPO/OOH and DMPO/H. In all samples, the relative intensity of the DMPO/H adduct was higher at the anode than at the cathode, suggesting the preferential generation of this adduct at the anode and leading us to propose the formation of $H^\bullet$ at the anode from the reaction of molecular hydrogen on the surface of the Pt catalyst, followed by spin trapping.

The generation of the DMPO/OOH adduct at the cathode was rationalized by H_2 crossover to the cathode, reaction at the Pt catalyst, and reaction with O_2. The DMPO/OOH adduct was also detected at the anode side. The presence of this adduct at the anode was explained by the reaction of crossover oxygen with hydrogen atoms formed at the anode Pt catalyst. The generation of the DMPO/OOH adduct depends therefore on gas crossover: at the cathode from crossover H_2 and at the anode from crossover O_2. As mentioned above, electrochemical generation of DMPO/OOH from H_2O_2, followed by reaction at the Pt catalyst, must also be considered for CCV conditions.

The DMPO/OH adduct was not detected in this study; however we cannot exclude the formation of this radical. The detection of DMPO/OOH at the cathode under OCV conditions may imply that the $HO^\bullet$ radical is formed chemically at the catalyst and reacts with the SPEEK ionomer. We note that the DMPO/OH adduct was detected at cathode OCV in the in situ ESR study of sulfonated poly(benzoyl paraphenylene) (SParmax).[7] It is possible that the diffusion-controlled reaction of $HO^\bullet$ with SParmax is slower than the corresponding reaction in SPEEK for the experimental conditions described here.

In SPEEK membranes directly exposed to hydroxyl radicals and in the presence of DMPO, the adducts detected were DMPO/Ph and DMPO/OPh,[31,32] indicating poor chemical stability of SPEEK in a Fenton test. In contrast to these *ex situ* experiments, no carbon-centered or oxygen-centered radical adducts were detected in the *in situ* FC. The results presented here show that, as mentioned in ref 19, hydrocarbon membranes may demonstrate different stability in the two tests and suggest that the membrane durability has to be evaluated under FC operating conditions.

Gas crossover is essential for the generation of short-lived species. The generation of the DMPO/OOH adduct depends on gas crossover, at the cathode from H_2 crossover, and at the anode from O_2 crossover. Rates of gas crossover depend on the degree of membrane hydration: the DMPO/H adduct was detected at the cathode CCV in the "wet" membrane, indicating H_2 crossover from the anode to the cathode; however, this adduct was absent in the "dry" membrane.

■ AUTHOR INFORMATION

Corresponding Author

*Tel 1-313-993-1012, Fax 1-313-993-1144, e-mail schlicks@udmercy.edu (S.S.).

Present Addresses

[§]On leave from the Institute of Nuclear Chemistry and Technology, Warsaw, Poland.

[‖]Global Fuel Cell Activities, 895 Joslyn Avenue, Pontiac, MI 48340.

Notes

The authors declare no competing financial interest.

■ ACKNOWLEDGMENTS

This study was supported by the Polymers Program of the National Science Foundation, by the General Motors Fuel Cell Activities Program, and by an unrestricted grant from University Research Program of Ford Motor Company. We are grateful to Dr. Cortney Mittelsteadt of Giner Electrochemical Systems LLC for the gift of MEAs based on SPEEK membranes. We are grateful to the two reviewers for their careful reading of the manuscript, interesting questions, and constructive criticism.

REFERENCES

(1) Kreuer, K. D.; Paddison, S. J.; Spohr, E.; Schuster, M. *Chem. Rev.* **2004**, *104*, 4637−4678.
(2) Mauritz, K. A.; Moore, R. B. *Chem. Rev.* **2004**, *104*, 4535−4585.
(3) Borup, R.; Meyers, J.; Pivovar, B.; Kim, R.; Mukundan, R.; Garland, N.; Meyers, D.; Wilson, M.; Garzon, F.; Wood, P.; et al. *Chem. Rev.* **2007**, *104*, 3904−3951.
(4) Johnson, B. C.; Yilgor, I.; Tran, C.; Iqbal, M.; Wightman, J. P.; Lloyd, D. R.; McGrath, J. E. *J. Polym. Sci., Polym. Chem. Ed.* **1984**, *22*, 721−737.
(5) Bae, B.; Miyatake, K.; Watanabe, M. *ECS Trans.* **2010**, *25*, 415−422.
(6) Lufrano, F.; Gatto, I.; Staiti, P.; Antonucci, V.; Passalacqua, E. *Solid State Ionics* **2001**, *145*, 47−51.
(7) Lancucki, L.; Schlick, S.; Danilczuk, M.; Coms, F. D.; Kruczala, K. *Polym. Degrad. Stab.* **2013**, *98*, 3−11.
(8) Xiao, L.; Zhang, H.; Scanlon, E.; Ramanathan, L. S.; Choe, E. W.; Rogers, D.; Apple, T.; Benicewicz, B. C. *Chem. Mater.* **2005**, *17*, 5328−5333.
(9) Bae, B.; Hoshi, T.; Miyatake, K.; Watanabe, M. *Macromolecules* **2011**, *44*, 3884−3892.
(10) Zhang, X.; Hu, Z.; Zhang, S.; Chen, S.; Chen, S.; Liu, J.; Wang, L. *J. Appl. Polym. Sci.* **2011**, *121*, 1707−1716.
(11) Bosnjakovic, A.; Schlick, S. *J. Phys. Chem. B* **2006**, *110*, 10720−10728.
(12) Danilczuk, M.; Coms, F. D.; Schlick, S. *J. Phys. Chem. B* **2009**, *113*, 8031−8042.
(13) Danilczuk, M.; Schlick, S.; Coms, F. D. *Macromolecules* **2009**, *42*, 8943−8949.
(14) Danilczuk, M.; Lancucki, L.; Schlick, S.; Hamrock, S. J.; Haugen, G. M. *ACS Macro Lett.* **2012**, 280−285.
(15) Curtin, D. E.; Lousenberg, R. D.; Henry, T. J.; Tangeman, P. C.; Tisack, M. E. *J. Power Sources* **2004**, *131*, 41−48.
(16) Zhou, C.; Guerra, M. A.; Qiu, Z. M.; Zawodzinski, T.; Schiraldi, D. A. *Macromolecules* **2007**, *40*, 8695−8707.
(17) Schiraldi, D. A.; Savant, D.; Zhou, C. *ECS Trans.* **2010**, *33*, 883−888.
(18) Coms, F. D. *ECS Trans.* **2008**, *16*, 235−255.
(19) Gittleman, C. S.; Coms, F. D.; Lai, Y. H. In *Polymer Electrolyte Fuel Cell Degradation*; Matthew, M., Mench, M., Eds.; Academic Press: Boston, 2012; pp 15−88.
(20) Kerres, J.; Ullrich, A.; Meier, F.; Häring, T. *Solid State Ionics* **1999**, *125*, 243−249.
(21) Jörissen, L.; Gogel, V.; Kerres, J.; Garche, J. *J. Power Sources* **2002**, *105*, 267−273.
(22) Kaliaguine, S.; Mikhailenko, S. D.; Wang, K. P.; Xing, P.; Robertson, G.; Guiver, M. *Catal. Today* **2003**, *82*, 213−222.
(23) Chang, J. H.; Park, J. H.; Park, G. G.; Kim, C. S.; Park, O. O. *J. Power Sources* **2003**, *124*, 18−25.
(24) Huang, R. Y. M.; Shao, P.; Burns, C. M.; Feng, X. *J. Appl. Polym. Sci.* **2001**, *82*, 2651−2660.
(25) Mecheri, B.; D'Epifanio, A.; Traversa, E.; Licoccia, S. *J. Power Sources* **2008**, *178*, 554−560.
(26) Kobayashi, T.; Rikukawa, M.; Sanui, K.; Ogata, K. *Solid State Ionics* **1998**, *106*, 219−225.
(27) Rikukawa, M.; Sanui, K. *Prog. Polym. Sci.* **2000**, *25*, 1463−1502.
(28) Kreuer, K. D. *J. Membr. Sci.* **2001**, *185*, 29−39.
(29) Xing, P. X.; Robertson, G. P.; Guiver, M. D.; Mikhailenko, S. D.; Wang, K. P.; Kaliaguine, S. *J. Membr. Sci.* **2004**, *229*, 95−106.
(30) Robertson, G. P.; Mikhailenko, S. D.; Wang, K.; Xing, P.; Guiver, M. D.; Kaliaguine, S. *J. Membr. Sci.* **2003**, *219*, 113−121.
(31) Hubner, G.; Roduner, E. *J. Mater. Chem.* **1999**, *9*, 409−418.
(32) Pinteala, M.; Schlick, S. *Polym. Degrad. Stab.* **2009**, *94*, 1779−1787.
(33) Lawrence, J.; Yamaguchi, T. *J. Membr. Sci.* **2008**, *325*, 633−640.
(34) Zhang, L.; Mukerjee, S. *J. Electrochem. Soc.* **2006**, *153*, A1062−A1072.
(35) Buchi, F. N.; Gupta, B.; Haas, O.; Scherer, G. G. *Electrochim. Acta* **1995**, *40*, 345−353.
(36) Chen, J.; Maekawa, Y.; Asano, M.; Yoshida, M. *Polymer* **2007**, *48*, 6002−6009.
(37) Kayser, M. J.; Reinholdt, M. X.; Kaliaguine, S. *J. Phys. Chem. B* **2011**, *115*, 2916−2923.
(38) Gode, P.; Ihonen, J.; Strandroth, A.; Ericson, H.; Lindbergh, G.; Paronen, M.; Sundholm, F.; Sundholm, G.; Walsby, N. *Fuel Cells* **2003**, *3*, 21−27.
(39) Chen, J.; Asano, M.; Maekawa, Y.; Yoshida, M. *J. Membr. Sci.* **2008**, *319*, 1−4.
(40) Janzen, E. G. *Acc. Chem. Res.* **1971**, *4*, 31−40.
(41) http://www.niehs.nih.gov/research/resources/software/toxpharm/tools/index.cfm.
(42) Rosen, G. M.; Beselman, A.; Tsai, P.; Pou, S.; Mailer, C.; Ichikawa, K.; Robinson, B. H.; Nielsen, R.; Halpern, H. J.; MacKerell, A. D. J. *J. Org. Chem.* **2004**, *69*, 1321−1330.
(43) Clement, J. L.; Ferre, N.; Siri, D.; Karoui, H.; Rockenbauer, A.; Tordo, P. *J. Org. Chem.* **2005**, *70*, 1198−1203.
(44) Villamena, F. A.; Merle, J. K.; Hadad, C. M.; Zweier, J. L. *J. Phys. Chem. A* **2005**, *109*, 6083−6088.
(45) Villamena, F. A.; Merle, J. K.; Hadad, C. M.; Zweier, J. L. *J. Phys. Chem. A* **2005**, *109*, 6089−6098.
(46) Danilczuk, M.; Coms, F. D.; Schlick, S. *Fuel Cells* **2008**, *8*, 436−452.
(47) Spulber, M.; Schlick, S. *J. Phys. Chem. A* **2010**, *114*, 6217−6225.
(48) Spulber, M.; Schlick, S.; Villamena, F. A. *J. Phys. Chem. A* **2012**, *116*, 8475−8483.
(49) Komarov, P. V.; Veselov, I. N.; Chu, P. P.; Khalatur, P. G.; Khokhlov, A. R. *Chem. Phys. Lett.* **2010**, *487*, 291−296 and references therein.
(50) Lawton, J. S.; Budil, D. E. *J. Membr. Sci.* **2010**, *357*, 47−53.
(51) Rosen, G. M.; Beselman, A.; Tsai, P.; Pou, S.; Mailer, C.; Ichikawa, K.; Robinson, B. H.; Nielsen, R.; Halpern, H. J.; MacKerell, A. D. J. *J. Org. Chem.* **2004**, *69*, 1321−1330.
(52) Taniguchi, H.; Madden, K. P. *J. Am. Chem. Soc.* **1999**, *121*, 11875−11879.
(53) Lin, L.; Danilczuk, M.; Schlick, S. *J. Power Sources* **2013**, *233*, 98−103.
(54) Mittelsteadt, C. K.; Liu, H. In *Handbook of Fuel Cells − Fundamentals, Technology and Applications*; Vielstich, W., Yokokawa, H., Gasteiger, H. A., Eds.; Wiley and Sons: New York, 2009; Vol. *5*, pp 345−358.
(55) Sakai, T.; Takenaka, H.; Torikai, E. *J. Electrochem. Soc.* **1986**, *133*, 88−92.